J|A|C|S ARTICLES

Published on Web 04/19/2010

Immobilizing Water-Soluble Dendritic Electron Donors and Electron Acceptors—Phthalocyanines and Perylenediimides—onto Single Wall Carbon Nanotubes

Uwe Hahn,[†] Sarah Engmann,[‡] Christian Oelsner,[‡] Christian Ehli,[‡] Dirk M. Guldi,*[,‡] and Tomas Torres*[,†]

Departamento de Química Orgánica, Universidad Autónoma de Madrid, 28049 Madrid, Spain, and the Department of Chemistry and Pharmacy and Interdisciplinary Center for Molecular Materials (ICMM), Friedrich-Alexander-Universität Erlangen-Nürnberg, Egerlandstrasse 3, 91058 Erlangen, Germany

Received January 10, 2010; E-mail: tomas.torres@uam.es; dirk.guldi@chemie.uni-erlangen.de

Abstract: The complementary use of spectroscopy and microscopy sheds light onto mutual interactions between semiconducting single wall carbon nanotubes (SWNT) and either a strong dendritic electron acceptor—perylenediimide—or a strong dendritic electron donor—phthalocyanine. Importantly, the stability of the perylenediimide/SWNT electron donor−acceptor hybrids decreases with increasing dendrimer generation. Two effects are thought to be responsible for this trend. With increasing dendrimer generation we enhance (i) the hydrophilicity and (ii) the bulkiness of the resulting perylenediimides. Both effects are synergetic and, in turn, lower the immobilization strength onto SWNT. Owing to the larger size of the phthalocyanines, phthalocyanine/SWNT electron donor−acceptor hybrids, on the other hand, did not reveal such a marked dependence on the dendrimer generation. Several spectroscopies confirmed that distinct ground- and excited-state interactions prevail and that kinetically and spectroscopically well-characterized radical ion pair states are formed within a few picoseconds.

Introduction

The considerable interest in carbon nanotubes (CNTs) is closely related to their intriguing properties including electrical and thermal conductivities, chemical stability, and mechanical strength, among others.[1] As a result, this relatively novel carbon allotrope has been proposed for applications such as energy conversion,[2] sensing,[3] actuators,[4] or biological applications.[5] Importantly, the efforts to exploit the favorable CNT properties in energy conversion[2] or electronic devices[6] are fundamentally connected to the ease of CNTs to play the role of an electron acceptor and/or electron donor. Accordingly, in recent years carbon nanotube-based nanohybrids/-conjugates formed by electron donor−acceptor systems have been the focus of attention.[2a] Association with electron-donor or -acceptors thereby assists in modulating the electronic properties of CNTs.

In terms of electron-donating materials, compounds based on macrocycles such as phthalocyanines represent a class for which attention emanates from their ability to harvest light and subsequently occurring energy- or electron transfer processes.[7] These planar molecules with an elongated electron-rich aromatic structure give rise to remarkably high extinction coefficients in the red and near-infrared region. Apart from this, they have been found to disclose outstanding photostability and singular physical properties. These features are the origin for phthalocyanines to be strongly investigated in recent years in various fields such as for photovoltaic devices.[8] The phthalocyanine moiety has also been in donor−acceptor systems together with fullerenes,[9] perylenes,[10] or related macrocyclic structures[11] to furnish long-lived and highly emissive charge-separated states. In line with these observations are species consisting of CNTs and phthalocyanines.[9a,12] On the other hand, perylene derivatives also represent a class of compounds with high photo- and

[†] Universidad Autónoma de Madrid.

[‡] Friedrich-Alexander-Universität Erlangen-Nürnberg.

(1) (a) Harris, P. J. F., Ed. *Carbon Nanotube Science: Synthesis, Properties and Applications*; Cambridge University Press: Cambridge, 2009. (b) Reich, S., Thomsen, C., Maultzsch, J., Eds. *Carbon Nanotubes: Basic Concepts and Physical Properties*; Wiley-VCH: Weinheim, 2004. (c) Jorio, A., Dresselhaus, G., Dresselhaus, M. S., Eds. *Carbon Nanotubes: Advanced Topics in the Synthesis, Structure, Properties and Applications*; Springer: Berlin, 2008. (d) Dresselhaus, M. S., Dresselhaus, G., Avouris, P., Eds. *Carbon Nanotubes: Synthesis, Structure, Properties and Applications*; Springer: Berlin, 2001.

(2) (a) Guldi, D. M.; Rahman, G. M. A.; Zerbetto, F.; Prato, M. *Acc. Chem. Res.* **2005**, *38*, 871. (b) Fischer, J. E. *Acc. Chem. Res.* **2002**, *35*, 19104. (c) Rahman, G. M. A.; Guldi, D. M.; Cagnoli, R.; Mucci, A.; Schenetti, L.; Vaccari, L.; Prato, M. *J. Am. Chem. Soc.* **2005**, *127*, 10051. (d) Umeyama, T.; Imahori, H. *Energy Environ. Sci.* **2008**, *1*, 120. (e) Tsakalakos, L. *Mater. Sci. Eng., R* **2008**, *62*, 175. (f) Guldi, D. M.; Rahman, G. M. A.; Sgobba, V.; Kotov, N. A.; Bonifazi, D.; Prato, M. *J. Am. Chem. Soc.* **2006**, *128*, 2315. (g) Somani, P. R.; Somani, S. P.; Umeno, M. *Appl. Phys. Lett.* **2008**, *93*, 033315. (h) Landi, B. J.; Castro, S. L.; Ruf, H. J.; Evans, C. M.; Bailey, S. G.; Raffaelle, R. P. *Sol. Energy Mater. Sol. Cells* **2005**, *87*, 733. (i) Raffaelle, R. P.; Landi, B. J.; Harris, J. D.; Bailey, S. G.; Hepp, A. F. *Mater. Sci. Eng., B* **2005**, *116*, 233. (j) Bhattacharyya, S.; Kymakis, E.; Amaratunga, G. A. J. *Chem. Mater.* **2004**, *16*, 4819. (k) Rolison, D. R.; Long, R. W.; Lytle, J. C.; Fischer, A. E.; Rhodes, C. P.; McEvoy, T. M.; Bourga, M. E.; Lubers, A. M. *Chem. Soc. Rev.* **2009**, *38*, 226.

(3) (a) Kauffman, D. R.; Star, A. *Angew. Chem., Int. Ed.* **2008**, *47*, 6550. (b) Ahammad, A. J. S.; Lee, J. J.; Rahman, M. A. *Sensors* **2009**, *9*, 2289. (c) Vichchulada, P.; Lipscomb, L. D.; Zhang, Q. H.; Lay, M. D. *J. Nanosci. Nanotechnol.* **2009**, *9*, 2189. (d) Sinha, N.; Ma, J. Z.; Yeow, J. T. W. *J. Nanosci. Nanotechnol.* **2006**, *6*, 573.

 10.1021/ja100065h

chemical stability, which in addition shows excellent electron-acceptor properties.[13] As valid as for the phthalocyanines, the extended aromatic system of perylenes with a fused five-ring π-system makes them susceptible for $\pi-\pi$ stacking onto the single wall carbon nanotubes (SWNT) surface by noncovalent interactions. Recently, we have demonstrated the assembly of perylene−SWNT nanohybrids, thus introducing one of the few examples in which the SWNT played the role of the electron donor.[14]

The solubilization or dispersion of phthalocyanine−CNT conjugates is crucial when aiming at investigating the materials properties of such assembled nanohybrids. However, many of the specimens at the early stage of research on CNTs appeared to be rather insoluble in common organic solvents. This point has been addressed in recent years by the development of synthetic strategies that allowed obtaining soluble derivatives, while at the same time preserving the tubular CNT structure.[15] Apart from the covalent modification of SWNT with phthalocyanine moieties,[9a,16] the noncovalent functionalization typically via $\pi-\pi$-interactions offers a potent means for the construction of donor−acceptor systems containing SWNT.[12a,15,17] Whereas the former approach most often has a significant impact on the SWNT materials properties, the latter has been demonstrated not to disrupt the conjugated electronic structure in nanotubes with minor influences on the particular SWNT features. However, a certain effect on the electronic transitions in the nanotubes has still to be considered. Hence, a viable solution-phase processability of such nanotube-based functional materials for example, in the fabrication and deposition into devices becomes achievable. Both approaches even have the potential for the development of CNT-based materials being soluble in water, thus enabling their processing under environmentally friendly conditions.

Herein, we report the preparation of new dispersible Pc−SWNT or perylene−SWNT nanohybrids. The employment

(4) (a) Mirfakhrai, T.; Madden, J. D. W.; Baughman, R. H. *Mater. Today* **2007**, *10*, 30. (b) Aliev, A. E.; Oh, J.; Kozlov, M. E.; Kuznetsov, A. A.; Fang, S.; Fonseca, A. F.; Ovalle, R.; Lima, M. D.; Haque, M. H.; Gartstein, Y. N.; Zhang, M.; Zakhidov, A. A.; Baughman, R. H. *Science* **2009**, *323*, 1575. (c) Ahir, S. V.; Terentjev, E. M. *Nat. Mater.* **2005**, *4*, 491. (d) Koerner, H.; Price, G.; Pearce, N. A.; Alexander, M.; Vaia, R. A. *Nat. Mater.* **2004**, *3*, 115. (e) Miaudet, P.; Derré, A.; Maugey, M.; Zakri, C.; Piccione, P. M.; Inoubli, R.; Poulin, P. *Science* **2007**, *318*, 1294. (f) Lu, S.; Panchapakesan, B. *Nanotechnology* **2005**, *16*, 2548. (g) Riemenschneider, J.; Temmen, H.; Monner, H. P. *J. Nanosci. Nanotechnol.* **2007**, *7*, 3359.

(5) (a) Tran, P. A.; Zhang, L. J.; Webster, T. J. *Adv. Drug Deliver. Rev.* **2009**, *61*, 1097. (b) Saito, N.; Usui, Y.; Aoki, K.; Narita, N.; Shimizu, M.; Hara, K.; Ogiwara, N.; Nakamura, K.; Ishigaki, N.; Kato, H.; Taruta, S.; Endo, M. *Chem. Soc. Rev.* **2009**, *38*, 1897. (c) Prato, M.; Kostarelos, K.; Bianco, A. *Acc. Chem. Res.* **2008**, *41*, 60. (d) Yang, W.; Thordarson, P.; Gooding, J. J.; Ringer, S. P.; Braet, F. *Nanotechnology* **2007**, *18*, 412001. (e) Bekyarova, E.; Ni, Y.; Malarkey, E. B.; Montana, V.; McWilliams, J. L.; Haddon, R. C.; Parpura, V. *J. Biomed. Nanotechnol.* **2005**, *1*, 3. (f) Katz, E.; Willner, I. *ChemPhysChem* **2004**, *5*, 1084. (g) Lin, Y.; Tailor, S.; Li, H.; Shiral Fernando, K. A.; Qu, L.; Wang, W.; Gu, L.; Zhou, B.; Sun, Y.-P. *J. Mater. Chem.* **2004**, *14*, 527. (h) Bianco, A.; Kostaleros, K.; Partidos, C. D.; Prato, M. *Chem. Commun.* **2005**, 571. (i) Kostaleros, K.; Lacerda, L.; Pastorin, G.; Wu, W.; Wieckowski, S.; Luangsivilay, J.; Godefroy, S.; Pantarotto, D.; Briand, J.-P.; Muller, S.; Prato, M.; Bianco, A. *Nat. Nanotechnol.* **2007**, *2*, 108. (j) Kam, N. W. S.; O'Connell, M.; Wisdom, J. A.; Dai, H. *Proc. Natl. Acad. Sci. U.S.A.* **2005**, *102*, 11600. (k) Kam, N. W. S.; Dai, H. *J. Am. Chem. Soc.* **2005**, *127*, 6021.

(6) (a) Sgobba, V.; Guldi, D. M. *Chem. Soc. Rev.* **2009**, *38*, 165. (b) Cao, Q.; Rogers, J. A. *Adv. Mater.* **2009**, *21*, 29. (c) Noy, A.; Artyukhin, A. B.; Misra, N. *Mater. Today* **2009**, *12*, 22. (d) Feldman, A. K.; Steigerwald, M. L.; Guo, X. F.; Nuckolls, C. *Acc. Chem. Res.* **2008**, *41*, 1731. (e) Balasubramanian, K.; Burghard, M. *J. Mater. Chem.* **2008**, *18*, 3071. (f) Avouris, P.; Chen, Z. H.; Perebeinos, V. *Nat. Nanotechnol.* **2007**, *2*, 605. (g) Liu, S.; Li, J.; Shen, Q.; Cao, Y.; Guo, X.; Zhang, G.; Feng, C.; Zhang, J.; Liu, Z.; Steigerwald, M. L.; Xu, D.; Nuckolls, C. *Angew. Chem., Int. Ed.* **2009**, *48*, 4759. (h) Fan, Z.; Ho, J. C.; Takahashi, T.; Yerushalmi, R.; Takei, K.; Ford, A. C.; Chueh, Y.-L.; Javey, A. *Adv. Mater.* **2009**, *21*, 3730.

(7) (a) Kadish, K. M., Smith, K. M., Guillard, R., Eds. *The Porphyrin Handbook*; Academic Press: San Diego, 2003; Vols. 15−20. (b) de la Torre, G.; Nicolau, M.; Torres, T. Phthalocyanines: Synthesis, Supramolecular Organization, and Photophysical Properties. In *Supramolecular Photosensitive and Electroactive Materials*; Nalwa, H. S., Ed.; Academic Press: New York, 2001; p 1. (c) de la Torre, G.; Claessens, C. G.; Torres, T. *Chem. Commun.* **2007**, 2000. (d) Rio, Y.; Rodríguez-Morgade, M. S.; Torres, T. *Org. Biomol. Chem.* **2008**, *6*, 1877. (e) Claessens, C. G.; Hahn, U.; Torres, T. *Chem. Rec.* **2008**, *8*, 75. (f) Tanaka, M. Phthalocyanines: High Performance Pigments and Their Applications. In *High Performance Pigments*; Faulkner, E. B., Schwartz, R. J., Ed.; Wiley-VCH: Weinheim, 2009, p 275. (g) de la Torre, G.; Bottari, G.; Hahn, U.; Torres, T. *Struct. Bond.* **2010**, *135*, 1.

(8) For some recent examples see: (a) Silvestri, F.; López-Duarte, I.; Seitz, W.; Beverina, L.; Martínez-Díaz, M. V.; Marks, T. J.; Guldi, D. M.; Pagani, G. A.; Torres, T. *Chem. Commun.* **2009**, 4500. (b) Morandeira, A.; López-Duarte, I.; O'Regan, B.; Martínez-Díaz, M. V.; Forneli, A.; Palomares, E.; Torres, T.; Durrant, J. R. *J. Mater. Chem.* **2009**, *19*, 5016. (c) Fischer, M. K. R.; López-Duarte, I.; Wienk, M. M.; Martínez-Díaz, M. V.; Janssen, R. A. J.; Bäuerle, P.; Torres, T. *J. Am. Chem. Soc.* **2009**, *131*, 8669. (d) Cid, J.-J.; García-Iglesias, M.; Yum, J.-H.; Forneli, A.; Albero, J.; Martínez-Ferrero, E.; Vázquez, P.; Grätzel, M.; Nazeeruddin, M. K.; Palomares, E.; Torres, T. *Chem.−Eur. J.* **2009**, *15*, 5130. (e) O'Regan, B. C.; López-Duarte, I.; Martínez-Díaz, M. V.; Forneli, A.; Albero, J.; Morandeira, A.; Palomares, E.; Torres, T.; Durrant, J. R. *J. Am. Chem. Soc.* **2008**, *130*, 2906. (f) Cid, J.-J.; Yum, J.-H.; Jang, S.-R.; Nazeeruddin, M. K.; Martínez-Ferrero, E.; Palomares, E.; Ko, J.; Grätzel, M.; Torres, T. *Angew. Chem., Int. Ed.* **2007**, *46*, 8358. (g) Morandeira, A.; López-Duarte, I.; Martínez-Díaz, M. V.; O'Regan, B.; Shuttle, C.; Haji-Zainulabidin, N. A.; Torres, T.; Palomares, E.; Durrant, J. R. *J. Am. Chem. Soc.* **2007**, *129*, 9250. Palomares, E.; Martínez-Díaz, M. V.; Haque, S. A.; Torres, T.; Durrant, J. R. *Chem. Commun.* **2004**, 2112.

(9) (a) Bottari, G.; de la Torre, G.; Torres, T.; Guldi, D. M. *Chem. Rev.* **2010**. Accepted for publication. (b) González-Rodríguez, D.; Bottari, G. *J. Porphyrins Phthalocyanines* **2009**, *13*, 624. (c) Rodríguez-Morgade, M. S.; Plonska-Brzezinska, M. E.; Athans, A. J.; Carbonell, E.; de Miguel, G.; Guldi, D. M.; Echegoyen, L.; Torres, T. *J. Am. Chem. Soc.* **2009**, *131*, 7727. (d) Pinzón, J. R.; Cardona, C. M.; Herranz, M. A.; Plonska-Brzezinska, M. E.; Palkar, A.; Athans, A. J.; Martin, N.; Rodríguez-Fortea, A.; Poblet, J. M.; Bottari, G.; Torres, T.; Gayathri, S. S.; Guldi, D. M.; Echegoyen, L. *Chem.−Eur. J.* **2009**, *15*, 864.

(10) (a) Rodríguez-Morgade, M. S.; Torres, T.; Atienza-Castellanos, C.; Guldi, D. M. *J. Am. Chem. Soc.* **2006**, *128*, 15145. (b) Jiménez, A. J.; Spänig, F.; Rodríguez-Morgade, M. S.; Ohkubo, K.; Fukuzumi, S.; Guldi, D. M.; Torres, T. *Org. Lett.* **2007**, *9*, 2481.

(11) (a) Claessens, C. G.; Torres, T. *Angew. Chem., Int. Ed.* **2002**, *41*, 2561. (b) González-Rodríguez, D.; Claessens, C. G.; Torres, T.; Liu, S.-G.; Echegoyen, L.; Vila, N.; Nonell, S. *Chem.−Eur. J.* **2005**, *11*, 3881. (c) Claessens, C. G.; Torres, T. *J. Am. Chem. Soc.* **2002**, *124*, 14522.

(12) (a) D'Souza, F.; Ito, O. *Chem. Commun.* **2009**, *33*, 4913. (b) de la Torre, G. *J. Porphyrins Phthalocyanines* **2009**, *13*, 637.

(13) Thompson, B. Perylene Pigments. In *High Performance Pigments*; Faulkner, E. B., Schwartz, R. J., Eds.; Wiley-VCH: Weinheim, 2009; p 261.

(14) Ehli, C.; Oelsner, C.; Guldi, D. M.; Mateo-Alonso, A.; Prato, M.; Schmidt, C.; Backes, C.; Hauke, F.; Hirsch, A. *Nat. Chem.* **2009**, *1*, 243.

(15) (a) Tasis, D.; Tagmatarchis, N.; Bianco, A.; Prato, M. *Chem. Rev.* **2006**, *106*, 1105. (b) Balasubramanian, K.; Burghard, M. *Small* **2005**, *1*, 180. (c) Sun, Y.-P.; Fu, K.; Lin, Y.; Huang, W. *Acc. Chem. Res.* **2002**, *35*, 1096.

(16) (a) Ballesteros, B.; de la Torre, G.; Ehli, C.; Rahman, G. M. A.; Agulló-Rueda, F.; Guldi, D. M.; Torres, T. *J. Am. Chem. Soc.* **2007**, *129*, 5061. (b) Ballesteros, B.; Campidelli, S.; de la Torre, G.; Ehli, C.; Guldi, D. M.; Prato, M.; Torres, T. *Chem. Commun.* **2007**, 2950. (c) Campidelli, S.; Ballesteros, B.; Filoramo, A.; Díaz Díaz, D.; de la Torre, G.; Torres, T.; Rahman, G. M. A.; Ehli, C.; Kiessling, D.; Werner, F.; Sgobba, V.; Guldi, D. M.; Cioffi, C.; Prato, M.; Bourgoin, J.-P. *J. Am. Chem. Soc.* **2008**, *130*, 11503. (d) de la Torre, G.; Blau, W.; Torres, T. *Nanotechnology* **2003**, *14*, 765.

(17) (a) Zhao, Y. L.; Stoddart, J. F. *Acc. Chem. Res.* **2009**, *42*, 1161. (b) Britz, D. A.; Khlobystov, A. N. *Chem. Soc. Rev.* **2006**, *35*, 637.

Chart 1

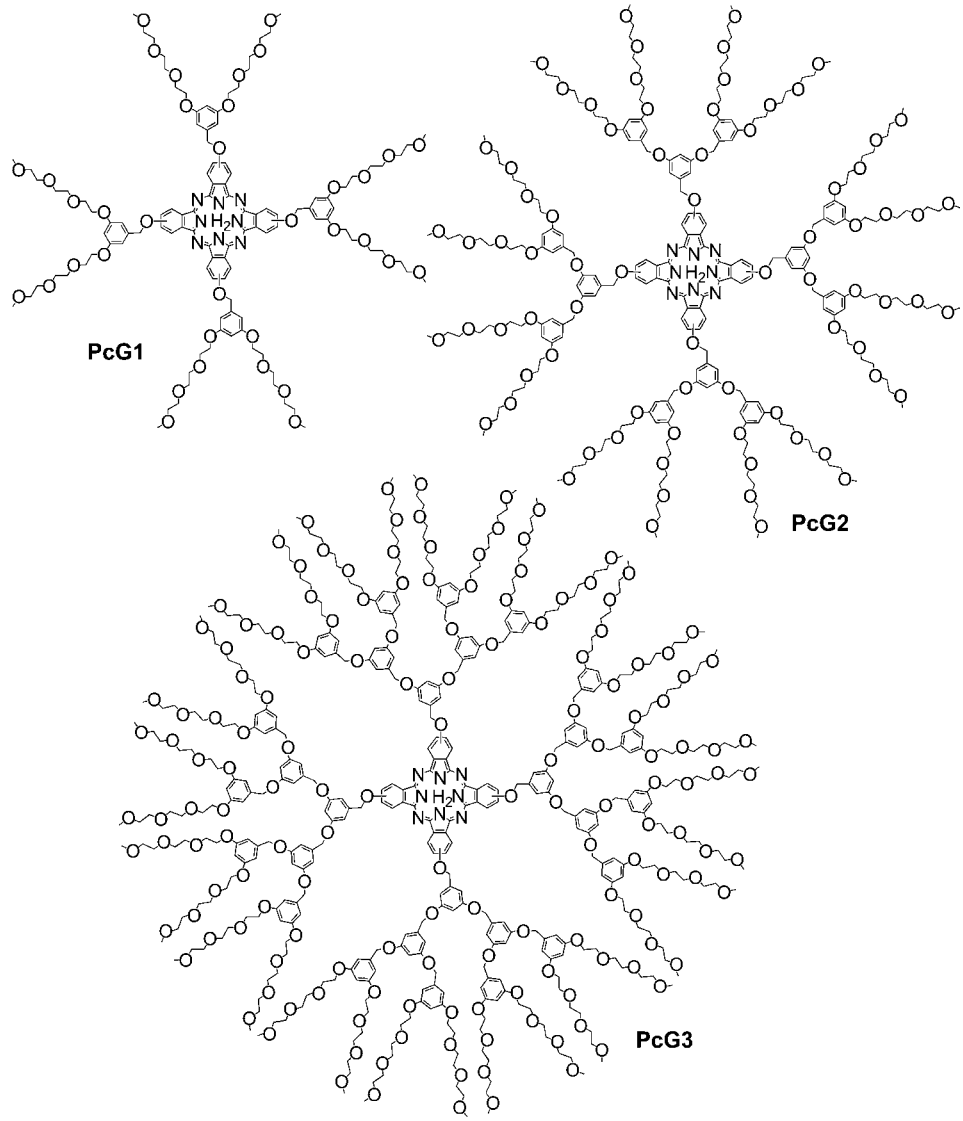

of dendritic structures with the hydrophobic phthalocyanine or perylene core moieties surrounded by an increasing number of oligoethylene glycol end groups allows for their dispersion and study in both common organic solvents and aqueous media. Selecting either a perylenediimide and/or a phthalocyanine offers the incentive of switching from an electron acceptor to an electron donor moiety as a potent means to manipulate the electronic properties of SWNT. The only requirement that the resulting conjugates—more specifically their cores—must meet is their adhesion to the SWNT surface. Notable is that this balance between hydrophobic and hydrophilic parts induces as well self-aggregation—vide infra. An in-depth photochemical study of the charge transfer chemistry of the series of Pc−SWNT and perylene−SWNT entities together with AFM and TEM images to disclose their macroscopic structures will be presented.

Results and Discussion

Synthesis. The dendritic free base phthalocyanines **PcG1**−**PcG3** (Chart 1) of first-to-third generations have been prepared according to the literature as described by McKeown et al.[18] The dendritic wedges of first-to-third generations with hydroxymethyl function were employed in aromatic nucleophilic substitution reactions between these materials and 4-nitrophthalonitrile to produce the required phthalonitriles in good to high yields of 50−80%. Finally, in each case dendrimer assembly was accomplished by the cyclotetramerization using lithium pentoxide in refluxing pentanol, to give **PcG1**−**G3** as a mixture of four inseparable isomers in 20−35% yield. The dendritic precursors **1**,**2**[19] of the first and second generations with triethylene glycol monomethyl ether end groups and benzylic bromide functions have also been the initial point for the synthesis of the preparation of the corresponding dendrons with amine functions. Consequently, reaction with sodium azide in

(18) (a) Brewis, M.; Helliwell, M.; McKeown, N. B.; Reynolds, S.; Shawcross, A. *Tetrahedron Lett.* **2001**, *42*, 813. (b) Brewis, M.; Helliwell, M.; McKeown, N. B. *Tetrahedron* **2003**, *59*, 3863.

(19) See for example: (a) Smith, D. K. *J. Chem. Soc., Perkin Trans. 2* **1999**, 1563. (b) Rio, Y.; Nicoud, J.-F.; Rehspringer, J.-L.; Nierengarten, J.-F. *Tetrahedron Lett.* **2000**, *41*, 10207. (c) Stephan, H.; Juran, S.; Born, K.; Comba, P.; Geipel, G.; Hahn, U.; Werner, N.; Vögtle, F. *New J. Chem.* **2008**, *32*, 2016.

Chart 2

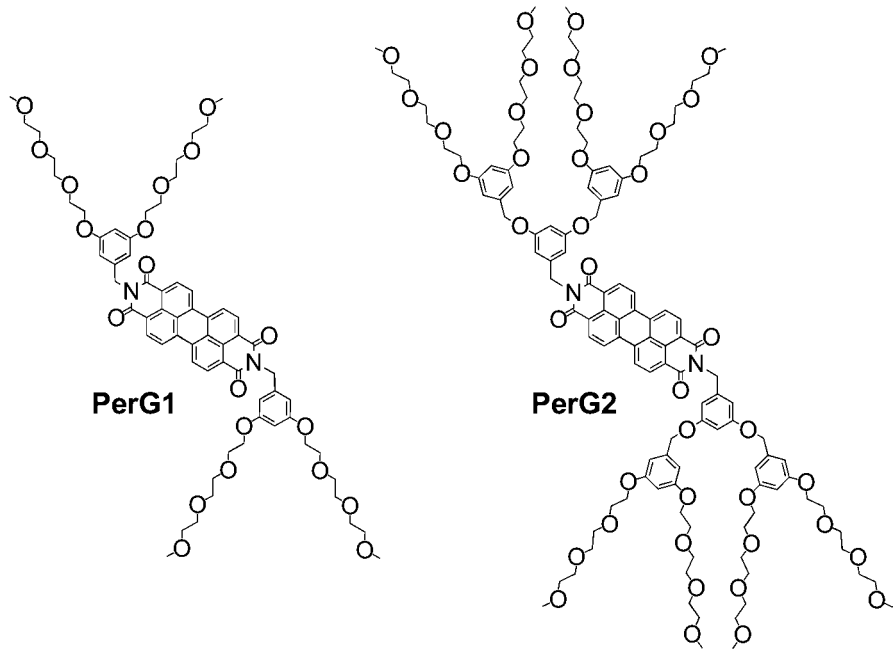

water provided quantitatively the corresponding benzylic azide derivatives **3**,**4**, which were then subjected to Staudinger reduction using triphenylphosphine in THF in the presence of traces of water to yield the targeted amines **5**,**6** as highly viscous liquids. These amino functions then served for the conjugation with perylene-3,4,9,10-tetracarboxylic dianhydride (**7**), which was accomplished in the presence of zinc acetate by heating a quinoline solution to 150 °C for 4 h. The target dendrimers **PerG1** and **PerG2** (Chart 2) were obtained in high yields of 87 and 89%, respectively, as intense red-colored solids after purification by column chromatography on silica gel and GPC. Owing to the ethylene glycol end groups both compounds are very soluble in common organic solvents such as CH_2Cl_2, $CHCl_3$, and THF. In addition, as a result of the high affinity of the multiple ethylene glycol termini toward water the greatest dendrimer **PerG2** is also readily soluble in aqueous medium. The increasing amount of hydrophilic surface moieties generates an amphiphilic environment in which the hydrophobic core is embedded as a center that is surrounded by the shell of peripheral oligoethylene glycol surface groups. It should be noted that **PerG2** has to be dissolved in water shortly after having been evaporated from an organic solution. Once reorganized in the solid state, this compound becomes marginally soluble in aqueous medium. However, employing the before-mentioned procedure to evaporating from an organic solution allows dissolving the substance in water.

The elucidation of all structures was easy, owing to the fact that the signals corresponding to the different parts of the dendrimers appear in specific regions. In particular, the protons of the perylene center appear as two signals located at 8.47 and 8.27 ppm. The NMR shifts for the dendritic part of the molecule are only significantly influenced at the methylene protons next to the bisimide function. These can be found at roughly 0.4 ppm downfield shifted when compared to the primary amines. As expected, the ^{13}C NMR spectra for the two dendrimers showed analogue shifts for the corresponding carbon atoms. The dendrimers were also characterized by MALDI-TOF mass spectrometry giving clean spectra with the target signals or adducts with sodium ions as base peaks (see Supporting Information).

Photophysical Characterization. First the physicochemical features of the different perylenediimides and phthalocyanines were tested in various media. Reasonable solubilities were ensured in toluene/dichloromethane (i.e., nonpolar) and water (i.e., polar) as the extreme scenarios.

In nonpolar solvents the absorption spectra of all dendritic perylenediimides **PerG1**−**2** and phthalocyanines **PcG1**−**3** are best described as monomers. In particular, for the perylenediimides **PerG1**−**2** (Figure 1) the characteristic 0−*2, 0−*1, and 0−*0 transitions were seen in the visible range with increasing oscillator strength at 460 nm < 490 nm < 529 nm. The phthalocyanines **PcG1**−**3**, on the other hand, reveal the corresponding 0−*2, 0−*1, and 0−*0 transitions at 645, 666, and 703 nm, again with increasing oscillator strength. Notably, the different dendron generations inflict little if any changes on the absorption features, and neither does a change in solvent polarity (i.e., toluene versus THF) lead to any appreciable effects. In all cases, emission spectra were recorded that mirror-image the aforementioned absorptions. For the perylenediimides 535 and 575 nm are the *0−0 and *0−1 maxima, while for the phthalocyanines the *0−0 maximum remained throughout the generations at 708 nm. Implicit are exceptionally small Stokes shifts, as the energetic difference between the long wavelength absorption and short wavelength fluorescence, which are on the order of 5−6 nm. The latter relate well with the rigid structures of the chromophores, preventing significant alteration of the vibrational fine-structure.

Despite these invariable absorption and emission features, a look at the actual quantum yields of fluorescence reveals that the perylenediimides must interact electronically. Here, a reference value of almost unity should be considered. In the current cases the quantum yields increase with dendrimer generation and increase with decreasing solvent polarity with values ranging from 0.8 (i.e., second generation in toluene) to 0.03 (i.e., first generation in dichloromethane). In line with this general trend are the fluorescence lifetimes that are as long as

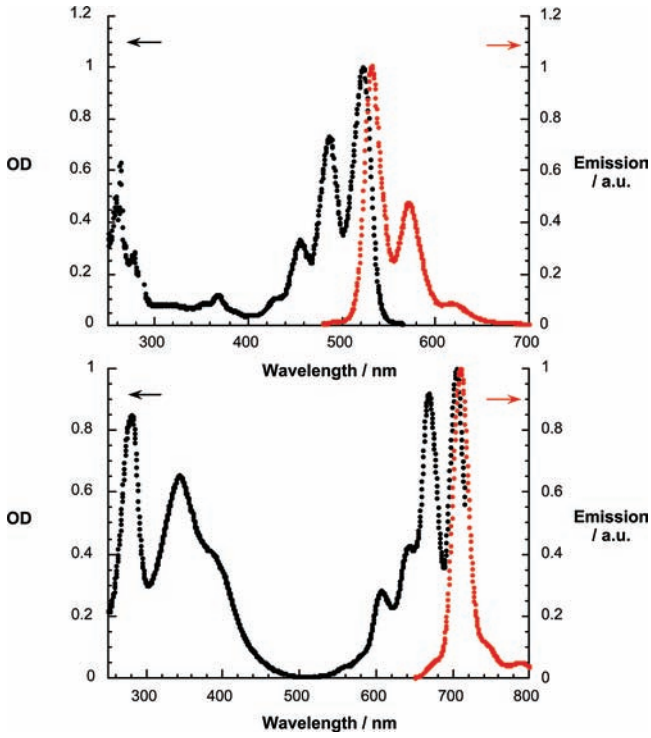

Figure 1. (Top) Excitation (i.e., black spectrum: 573 nm emission wavelength) and emission (i.e., red spectrum: 470 nm excitation wavelength) spectra of **PerG1** (4.3×10^{-6} M) in aerated THF solution at room temperature. (Bottom) Excitation (i.e., black spectrum: 720 nm emission wavelength) and emission (i.e., red spectrum: 633 nm excitation wavelength) spectra of **PcG3** (1.7×10^{-6} M) in aerated THF solution at room temperature.

2.5 ns and as short as <100 ps (i.e., the time-resolution of our setup). The phthalocyanine fluorescence, on the other hand, seems not to be affected at all, with quantum yields of 0.33 ± 0.06 and lifetimes of 6.2 ± 0.4 ns in toluene, THF, and dichloromethane.

In the corresponding transient absorption measurements, where we used approximately 150 fs pulse width excitation, we note the instantaneously formed singlet−singlet features of the perylenediimides (Figure S7, Supporting Information).[20] These include transient minima at 460, 490, and 530 nm of increasing strength, which indicate consumption of the ground state, and transient maxima at 720, 875, and 950 nm. A general feature of perylenediimides is their inefficient intersystem crossing as the instantaneously formed excited state deactivates nearly quantitatively via the radiative pathway to the ground state.[21] In this context, the singlet excited-state deactivation tracks the trend established in the time-resolved fluorescence measurements with lifetimes as short as 1750 ps: **PerG1** in THF. Likewise, the singlet excited-state features of the phthalocyanines evolve in 450−550 nm range as a broad transient maximum, in the 600−750 nm range as sharp bleaching (645, 665, and 703 nm) of the ground-state transitions and in the

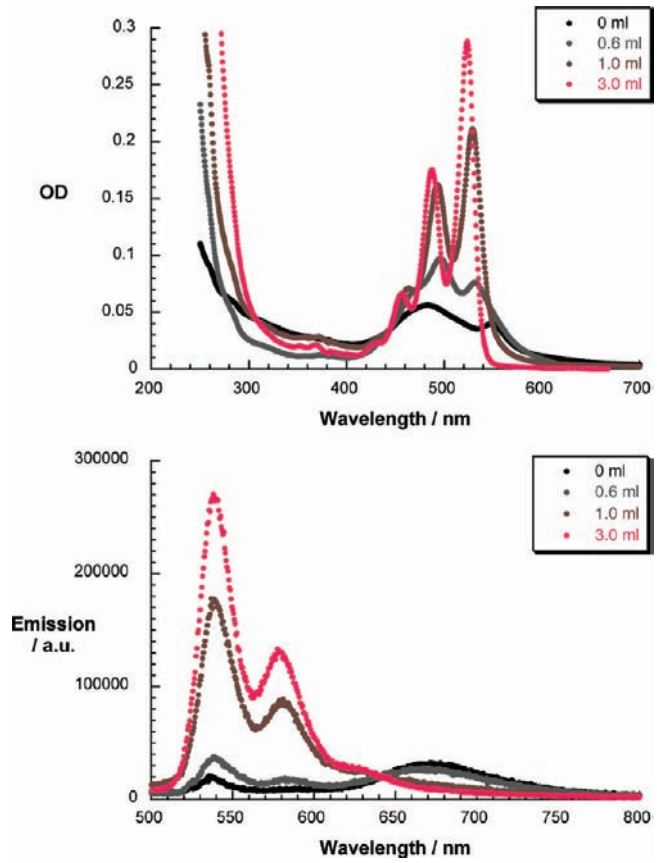

Figure 2. (Top) Steady-state absorption spectra of **PerG1** (3.3×10^{-6} M) in H_2O at room temperature in the absence and presence of variable amounts of THF (i.e., pure water - black; and pure THF - pink; and THF/water ratios of 1:4, 0.7:2.3, and 1:3). (Bottom) Emission spectra of **PerG1** (3.3×10^{-6} M) in H_2O at room temperature upon excitation at 450 nm in the absence and presence of variable amounts of THF (i.e., pure water - black; pure THF - pink; and THF/water ratios of 1:4, 0.7:2.3, and 1:3).

800−1300 nm range as a broad transient maximum (Figure S8, Supporting Information). Interestingly, for THF the singlet decay, which implies an intersystem crossing to the corresponding triplet manifold, depends on the dendrimer generation. Overall a stabilizing trend, that is, longer singlet excited-state lifetimes, evolves as the dendrimer generation increases: **PcG1** (630 ps) < **PcG2** (940 ps) < **PcG3** (1750 ps).

Although all of the tested perylenediimides and phthalocyanines were readily soluble in water, their absorption and fluorescence features differ fundamentally from the conclusions drawn from experiments in organic solvents. In organic media just the perylenediimide fluorescence prompts sizable interactions. Now in water perylenediimides and phthalocyanines are susceptible to changes in absorption as well as in fluorescence (!). At first glance the absorption spectra tend to reveal significant broadenings, when compared to those in, for example, toluene. A closer look sheds more light onto the underlying phenomena. In particular, in water the 0−*2, 0−*1, and 0−*0 transitions of the perylenediimides are red-shifted and reversed in oscillator strength, a clear indication of perylenediimide aggregation through the formation of electronically interacting *J*-aggregates, Figure S9, Supporting Information. In a decisive titration experiment the solvent polarity was changed more steadily, from pure THF step-by-step to that of almost utter water, Figure 2. A THF solution of perylenediimide (10^{-6} M) with 488 and 523 nm maxima was taken, and the water content was increased gradually, while keeping the concentration

(20) Weiss, E. A.; Ahrens, M. J.; Sinks, L. E.; Gusev, A. V.; Ratner, M. A.; Wasielewski, M. R. *J. Am. Chem. Soc.* **2004**, *126*, 5577.
(21) (a) Margineanu, A.; Hofkens, J.; Cotlet, M.; Habuchi, S.; Stefan, A.; Qu, J.; Kohl, C.; Müllen, K.; Vercammen, J.; Engelborghs, Y.; Gensch, T.; De Schryver, F. C. *J. Phys. Chem. B* **2004**, *108*, 12242. (b) Hayes, R. T.; Wasielewski, M. R.; Gosztola, D. *J. Am. Chem. Soc.* **2000**, *122*, 5563. (c) Kaletaş, B. K.; Dobrawa, R.; Sautter, A.; Würthner, F.; Zimine, M.; De Cola, L.; Williams, R. M. *J. Phys. Chem. A* **2004**, *108*, 1900.

constant. Throughout these experiments an isosbestic point developed at 448 nm. Moreover, an overall weakening of the absorption developed by approximately a factor of 4, a significant broadening that extended to ~650 nm, and a red-shift in water of all of the transitions evolved. Concurrently the monomer fluorescence, when exciting at the isosbestic point at 448 nm, underwent changes. This is in agreement with what has been seen in numerous cases for perylenediimide aggregates.[22] In fact, the rather sharp/strong maxima in the blue (i.e., maxima at 535 and 575 nm) are replaced by a broad/weak maximum in the red (i.e., maxima at 660 nm for **PerG1** or at 680 nm for **PerG2**). Nevertheless, a significant reduction in fluorescence quantum yields, 0.8 in organic media and 0.001 (**PerG1**)/0.002 (**PerG2**) in water, is associated with this transformation. In parallel with the absorption an isosbestic point, that is, a wavelength of equal fluorescence, emerges at 645 nm. Importantly, in time-resolved fluorescence measurements the aggregated forms of **PerG1** and **PerG2** give rise to lifetimes of 240 and 630 ps, respectively. In summary, fluorescence quantum yields track the fluorescence lifetimes reasonably well.

Finally, when contrasting the features of phthalocyanines in water with those in toluene, a similar trend, namely red-shifted and weakened absorptions, is discernible (Figure S10, Supporting Information). Please compare maxima for the aggregates at 601, 622, 696, and 745 nm with those of the monomers at 645, 666, and 703 nm. Fluorescence (i.e., quantum yields $\ll 10^{-4}$), on the other hand, was not seen at all for the phthalocyanines in water. This encouraged us to attempt the disaggregation by adding a surface-active surfactant, sodium dodecylbenzenesulfonate (SDBS), from which we expected to form a more homogeneous shield around the phthalocyanine. Indeed, features like those found in toluene as they evolve in the absorption and fluorescence spectra corroborate our assumption, that is, the quantitative recovery of what is assumed to be the monomer absorption and fluorescence spectra.

Transient absorption changes associated with the perylenediimides in water are quantitatively similar to our findings in nonpolar media. Specifically, we note minima at 490/530/575 nm and maxima at 680/810/1040 nm. It is, however, the relative intensities of these minima and maxima that are drastically different. To illustrate this, the minima intensities drop in the following order: 490 > 530 > 575 nm. Again, this finding suggests the formation of aggregates in water. The lifetimes of the perylenediimide singlet excited states are also affected by the aqueous environment. The values are as short as 200 ps for **PerG1**.

In the corresponding femtosecond experiments with the phthalocyanines, we note a trend that strongly resembles that seen in THF, Figure 3. In particular, the singlet excited state features with maxima in the 400−475 and 775−1300 nm regions and minima at 610 and 700 nm transform with lifetimes that depend on the dendrimer generation into those associated with the triplet manifold.

In summary, we have developed a series of spectroscopic features that assist in distinguishing between truly monomeric forms of perylenediimides and phthalocyanines and their corresponding aggregates. Important is their distinct tendency to adhere to each other, which leads to electronically interacting

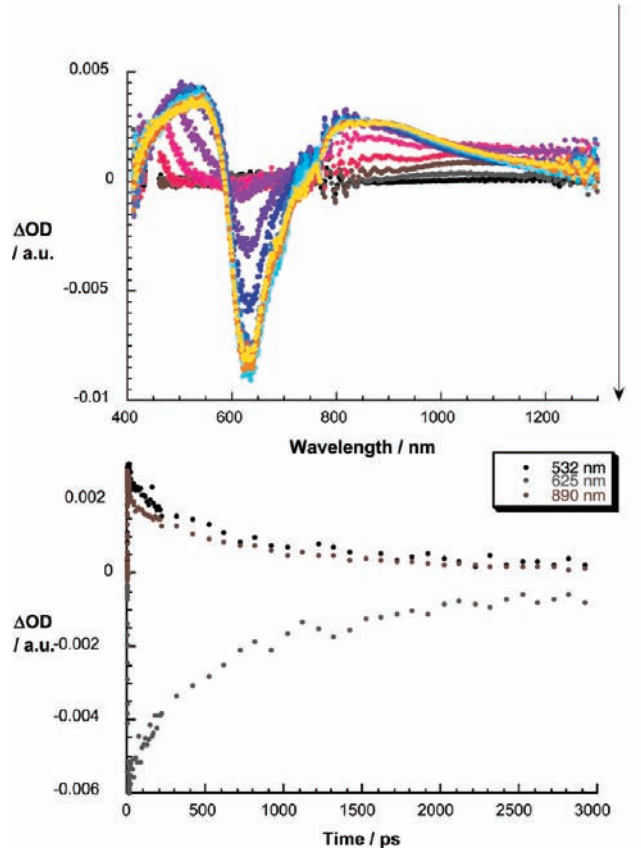

Figure 3. (Top) Differential absorption spectra (visible and near-infrared) obtained upon femtosecond flash photolysis (387 nm) of **PcG3** (4.0×10^{-5} M) in D_2O with several time delays between 0 and 3000 ps at room temperature; see figure legend for details about the time progression. (Bottom) Time-absorption profiles of the femtosecond spectra at 532, 625, and 890 nm, monitoring the intersystem crossing.

aggregates. This criterion is thought to be beneficial for the immobilization of the perylenediimides and phthalocyanines onto CNTs in general, vide infra. In the following, the aforementioned fingerprints are exploited as a way to characterize perylenediimide/SWNT and phthalocyanine/SWNT.

First, titration experiments with perylenediimides and SWNT, Figure 4, brought the following spectroscopic changes to light. In the visible range the perylenediimide-centered transitions (i.e., 483 and 548 nm) shift gradually to the red (i.e., 480, 520, and 560 nm) reflecting interactions between the perylenediimides and SWNT. It is notable that, when inspecting the relative ratios of the perylenediimide transitions at the beginning (483 nm > 548 nm) and at the end of the titration (520 nm < 560 nm), a trend is deduced, suggesting that individual perylenediimides have been exfoliated out of the initially formed aggregates and immobilized onto SWNT. We must assume that perylenediimides/SWNT interactions made up by contributions from $\pi-\pi$ stacking, hydrophobic forces, and charge transfer character prevail over those that just govern perylenediimide/perylenediimide interactions. Still, a comparison with the data taken in THF and/or an aqueous environment containing SDBS implies a significant red-shift, 25 nm, which relates to the adhesion onto SWNT. In the near-infrared range, the typical van Hove singularities of SWNT emerge. However, in contrast to a previous report the shifts are (i) to longer wavelengths and (ii) to moderate wavelengths (i.e., ~4 nm). As a matter of fact, ground-state interactions as a reflection of partial reduction of the perylenediimides and the simultaneous p-doping of SWNT

(22) For example: (a) Würthner, F.; Chen, Z.; Dehm, V.; Stepanenko, V. *Chem. Commun.* **2006**, 1188. (b) Jancy, B.; Asha, S. K. *Chem. Mater.* **2008**, *20*, 169.

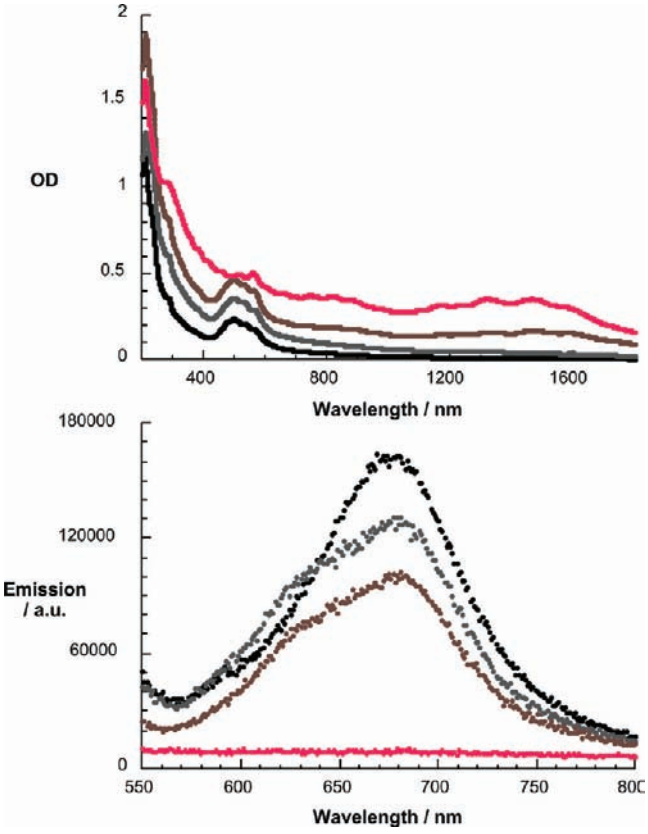

Figure 4. (Top) Steady-state absorption spectra of **PerG2** and **PerG2**/SWNT by stepwise increasing (black, gray, brown, and red) the SWNT concentration in D_2O. The concentration of **PerG2** is kept constant for all experiments (6.0×10^{-6} M). (Bottom) Complementary emission spectra of **PerG2** and **PerG2**/SWNT upon excitation at 480 nm.

are weak. This trend is also seen in the stability of the corresponding suspensions.

Insights into perylenediimide/SWNT interactions came from RAMAN experiments. Here, the two most important signatures, that is, RBM- and G-modes, reveal upshift from 266 and 1590 cm^{-1} to 270 and 1592 cm^{-1} in D_2O suspensions of SDBS/SWNT and perylenediimides/SWNT, respectively, as well in the solid without evident loss in resonance. This indicates the fact that $\pi-\pi$ interactions are operative. Augmentation through ground-state charge transfer/p-doping plays, however, only a minor role, if any.

Next, we turned to fluorescence as a complement to the aforementioned absorption assays. The most important observation is that the aggregate emission in the 550−800 nm range fades away gradually in the presence of SWNT without revealing sizable monomer fluorescence. It is safe to assume that in perylenediimide/SWNT the strong perylenediimide fluorescence is quenched due to thermodynamically favored charge- or energy transfer deactivations. Monomer fluorescence is only seen when SDBS is finally added. In this context, SDBS plays a key role in recovering the intrinsic fluorescence of the perylenediimides. Similarly, the original absorption features of perylenediimides and SWNT are progressively recovered. As a matter of fact, plotting the absorption changes at 557 nm (i.e., maximum changes due to the disappearance of perylenediimide/SWNT) and 530 nm (i.e., maximum changes due to the appearance of perylenediimides plus SWNT) as a function of

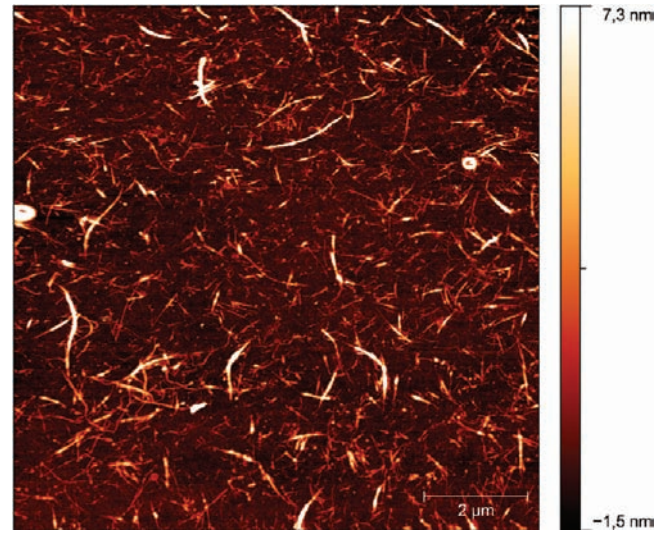

Figure 5. AFM image of **PerG2**/SWNT dispersion (D_2O).

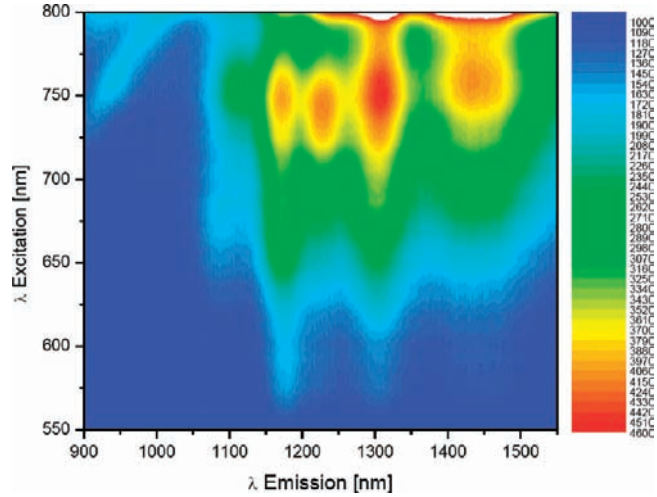

Figure 6. Steady-state fluorescence spectra, with increasing intensity from blue to green to yellow and to red, of **PerG1**/SWNT in D_2O dispersion.

SDBS concentrations, varying from 0.0 to 0.1 M, confirms the quantitative removal of the perylenediimides from the SWNT surface.

Ensuring the homogeneity of perylenediimide/SWNT is critical. Atomic force and transmission electron microscopies are important, since they provide important insights into this aspect. Throughout the scanned areas predominantly short (i.e., 500 μm) and thin bundles (i.e., 10 nm) are discernible; Figure 5.

Three-dimensional (3D) fluorescence landscapes were generated for SWNT/SDBS resembling those seen in previous reports. SWNT/SDBS exhibits the strongest fluorescence maxima from SWNT that are ascribed to (9,4), (7,6), (8,6), (11,3), (9,5), (10,5), (8,7), and (9,7), not shown. For **PerG1**/SWNT, Figure 6, a fluorescence pattern evolves with bathochromic changes when compared to SWNT/SDBS. For example, the 1108, 1180, and 1266 nm maxima shift to 1173, 1231, and 1313 nm, respectively. Importantly, considering the 1200−1600 nm range, the SWNT fluorescence is on the order between 10 and 14% when compared to that of SWNT/SDBS.

Transient absorption spectroscopy was employed to confirm the ultrafast singlet excited state deactivations and, in addition, to characterize the nature of the photoproducts. In measurements

with perylenediimide/SWNT (i.e., **PerG1**/SWNT and **PerG2**/SWNT) 387, 560, and 775 nm were selected as excitation wavelengths; 387 nm is rather unselective owing to the overlapping absorption of perylenediimides and SWNT in this range, while 560 and 775 nm enable the nearly selective excitation of perylenediimides and SWNT, respectively. Important is the detection of the rapidly formed singlet excited states of perylenediimides and SWNT. For the perylenediimides it is reassuring to see the 480, 520, and 560 nm characteristics, correlating with the red-shifted ground-state absorption of perylenediimide/SWNT rather than those at 460, 490, and 530 nm, due to the absorption of monomeric perylenediimides. SWNT, on the other hand, are distinguished by 950, 1160, 1318, 1465, and 1555 nm transitions. Both singlet excited states are, however, very short-lived as they deactivate in perylenediimide/SWNT within the first 5 ps following photoexcitation. Simultaneous with the excited-state decays, evolution of a new product is registered that in all of the cases includes perylenediimide- and SWNT-centered features. It is striking that these evolve despite the selective perylenediimide (i.e., 560 nm) or SWNT (i.e., 775 nm) excitation. This per se attests to the formation of what could be an energy transfer or a charge transfer product. A closer look at the features assists in identifying the nature of the photoproduct. At a delay time of 5 ps the following characteristics dominate the differential absorption changes. In the visible range these are a minimum at 555 nm and a maximum at 660 nm, which are clear attributes of the one-electron reduced form of perylenediimides as generated electrochemically and pulse radiolytically.[14] In the near-infrared region, appreciable blue-shifts of the transient bleaches with minima at 880 (i.e., from 900 nm), 958 (i.e., 962 nm), 1145 (i.e., from 1160 nm), 1285 (i.e., from 1318 nm), 1435 nm (i.e., from 1465 nm), and 1550 nm (i.e., from 1555 nm) are detected during the deactivation. We imply here the oxidized form of SWNT, in which the corresponding transitions are shifted to higher energies. In other words, we have established unambiguous evidence for charge separation that occurs from either photoexcited perylenediimides or photoexcited SWNT. In line with closely spaced entities the charge separated states are relatively short-lived. From a multiwavelength analysis we derived lifetimes of 120 and 160 ps for **PerG1**/SWNT and **PerG2**/SWNT, respectively. Figure 7 documents the growth and decay kinetics of the charge separated state.

In contrast, evidence for phthalocyanines that are interacting with SWNT was first gathered in THF. When THF was added to suspended SWNT solid probes of phthalocyanines, the successive growth of the phthalocyanine-centered transitions was observed at 668 and 703 nm. When inspecting the near-infrared section of the spectrum, where the SWNT-centered features appear, the underlying van Hove singularities further resembled that trend in the form of a red-shift. This corroborates the spontaneous immobilization of phthalocyanines onto SWNT.

In water, on the other hand, phthalocyanines (10^{-5} M) were blended with solid SWNT. Throughout this process, the broad features of the phthalocyanine aggregates disappeared between 500 and 800 nm and gave way to a 730 nm maximum. We tentatively assigned this sharp peak to that of monomeric phthalocyanines, albeit its location is in a range that is dominated by the van Hove singularities of SWNT. An unusually strong red-shift (i.e., 705 to 730 nm) that inflicts strong electronic interactions between phthalocyanines and SWNT driven by $\pi-\pi$ and charge transfer forces would be implicit. Confirmation for this assignment came from attempts to replace the phthalocyanines by SDBS. The corresponding experiments at room temperature were unsuccessful, however, owing to the strong adhesion forces that necessitate a significant

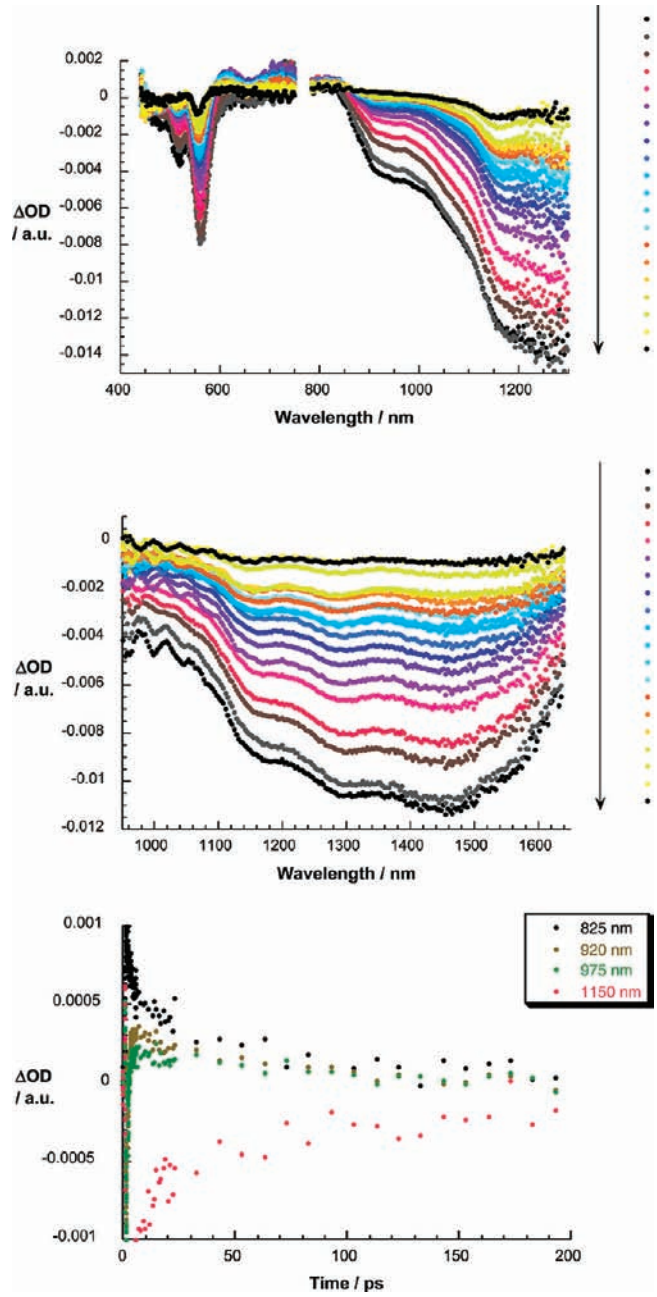

Figure 7. (Top) Differential absorption spectra (visible and near-infrared) obtained upon femtosecond flash photolysis (387 nm) of **PerG1**/SWNT in D_2O with several time delays between 0 and 200 ps at room temperature; see figure legend for details about the time progression. (Center) Differential absorption spectra (extended near-infrared) obtained upon femtosecond flash photolysis (387 nm) of **PerG1** /SWNT in D_2O with several time delays between 0 and 200 ps at room temperature; see figure legend for details about the time progression. (Bottom) Time-absorption profiles of the femtosecond spectra at 825, 920, 975, and 1150 nm, monitoring the charge separation and charge recombination.

activation barrier. This trend is also exemplified by the remarkable stability of the phthalocyanine/SWNT suspensions that even after months failed to give rise to any detectable changes. To overcome the apparent activation barrier for desorbing the phthalocyanines from SWNT, heat (i.e., up to 60 °C) was applied. Indeed, under these conditions the known maxima of phthalocyanines in THF and/or water plus SDBS, vide supra, evolve at 665 and 705 nm. The transformation (i.e., 730 to 665/705 nm) is, however, incomplete and is indicative of an equilibrium that even at elevated

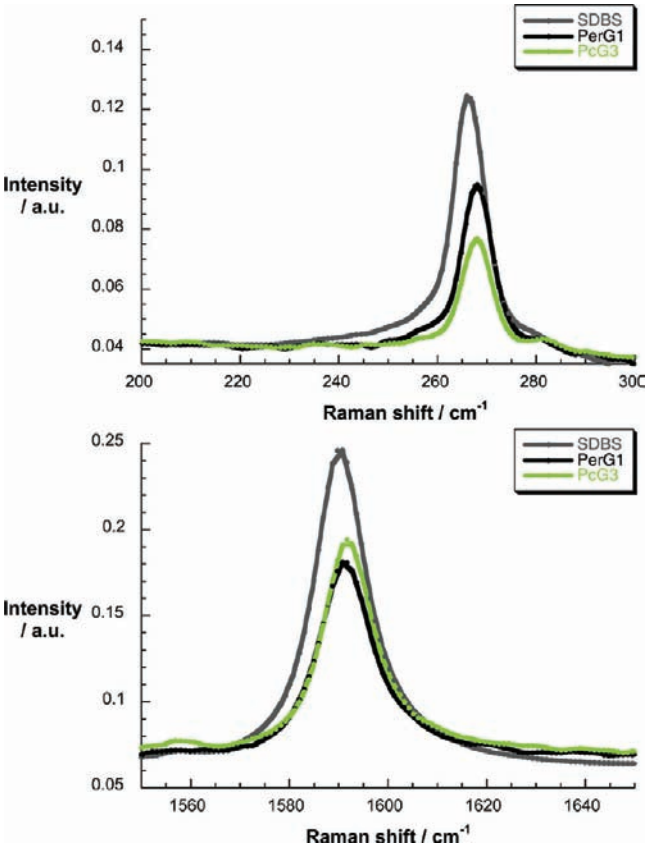

Figure 8. Raman spectra of SWNT/SDBS (gray spectrum), **PerG1**/SWNT (black spectrum), and **PcG3**/SWNT (green spectrum).

temperatures is not fully pushed back to the side of free phthalocyanines plus SWNT.

Raman experiments (see Figure 8) confirm that, for phthalocyanine/SWNT, as in the case of perylenediimide/SWNT, $\pi-\pi$ interactions are decisive. In particular, relative to SDBS/SWNT, the RBM- and G-modes upshift in perylenediimides/SWNT from 266 and 1590 cm^{-1} to 269 and 1592 cm^{-1}, respectively (i.e., D_2O suspensions and in the solid). Ground-state charge transfer/n-doping, on the other hand, seems to play no significant role.

AFM and TEM confirm the presence of SWNT in phthalocyanine/SWNT. Representative images reveal objects with high aspect ratio that appear throughout the scanned regions, Figure 9. The mean length of these objects is typically on the order of several micrometers, and their diameters range between a few nanometers and several tens of nanometers.

Charge transfer processes evolving from either photoexcited phthalocyanines or SWNT were probed in steady-state fluorescence experiments in THF as solvent. To this end, the fluorescence of phthalocyanines at 708 nm was compared in the absence and presence of SWNT. Of relevance is a significant quenching of phthalocyanine fluorescence in phthalocyanine/SWNT. Filter effects (i.e., SWNT absorption, etc.) should not be ruled out as a sensible contribution to the quantitative quenching.

For phthalocyanine/SWNT a fluorescence pattern evolves with bathochromic changes, when compared to SWNT/SDBS, which parallel those seen in the absorption spectrum, Figure 10. For example, the 1108 and 1180 nm maxima shift to 1140 and 1210 nm, respectively. An additional characteristic is that in the 1000 to 1550 nm range, the SWNT fluorescence is on

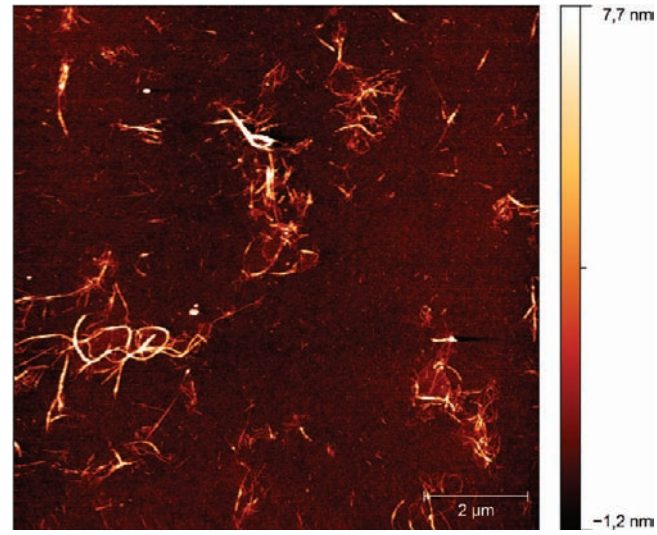

Figure 9. AFM image of **PcG3**/SWNT dispersion (D_2O).

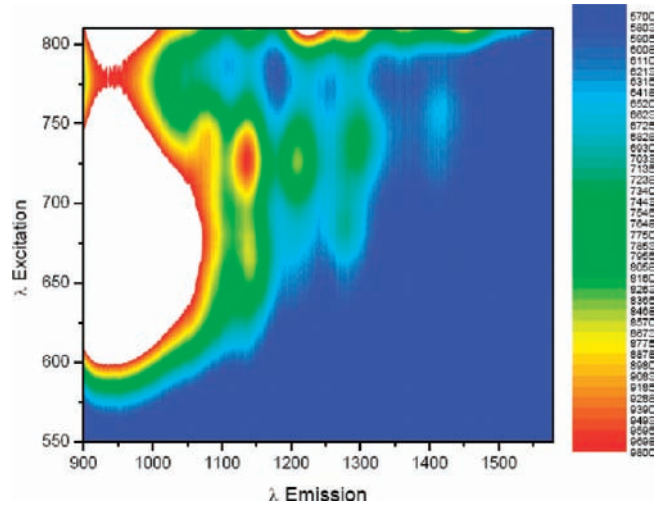

Figure 10. Steady-state fluorescence spectra, with increasing intensity from blue to green to yellow and to red, of **PcG3**/SWNT in D_2O dispersion.

the order between 14 and 23% when compared to that of SWNT/SDBS.[23] In line with what we have seen in the absorption measurements, addition of SDBS led to the expected blue-shift of the fluorescence peaks. Additionally, the intrinsic fluorescence intensity of SWNT/SDBS is partially recovered.

Finally, transient absorption measurements were performed with phthalocyanine/SWNT, see Figure 11. Here, 660 and 775 nm excitation wavelengths were used in addition to 387 nm to address the phthalocyanines and SWNT individually. Sufficient stability was, however, only observed for **PcG2**/SWNT and **PcG3**/SWNT, which, in turn, omitted investigations with **PcG1**/SWNT. Depending on the excitation wavelength we monitored how either the phthalocyanine or SWNT or both singlet excited states transform into the same photoproduct. For example, upon 660 nm the **PcG3** excited-state features are discernible in the 400−550 nm region. These decay, however, instantaneously (i.e., in less than 2 ps) to afford the charge transfer product. Spectroscopic proof for a charge transfer product was lent from the differential changes in the visible spectrum. Maxima at 530 and

(23) It is notable that the phthalocyanine fluorescence supersedes the SWNT fluorescence in some parts.

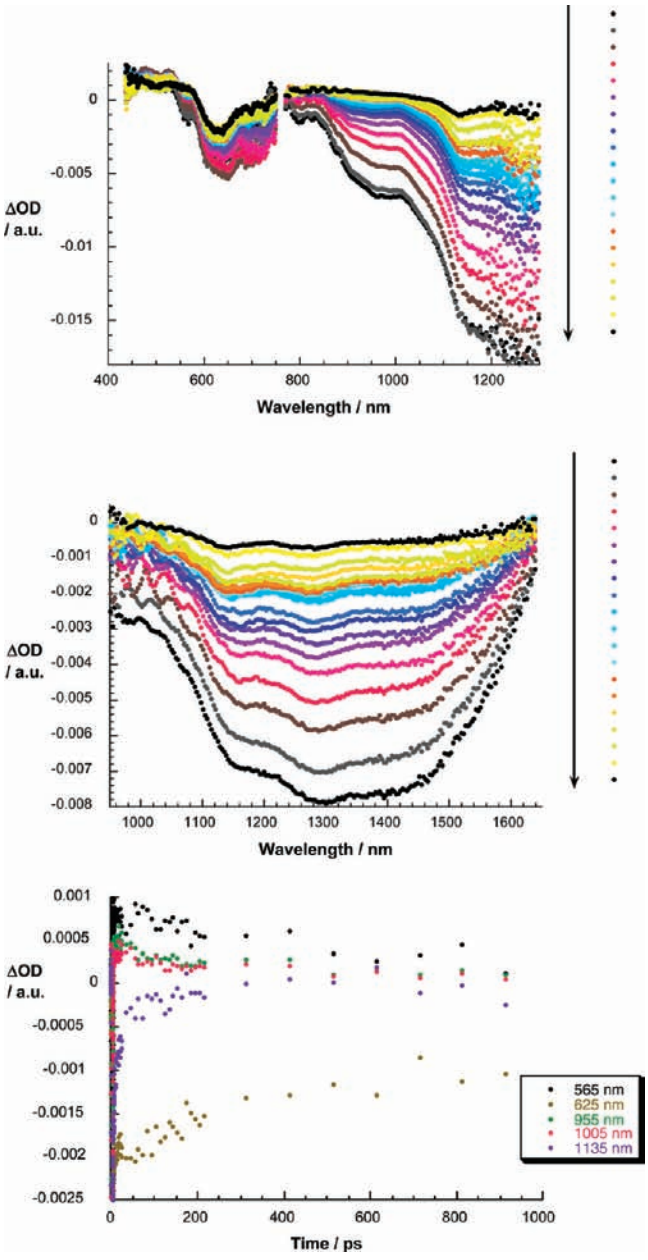

Figure 11. (Top) Differential absorption spectra (visible and near-infrared) obtained upon femtosecond flash photolysis (387 nm) of **PcG3**/SWNT in D_2O with several time delays between 0 and 200 ps at room temperature; see figure legend for details about the time progression. (Center) Differential absorption spectra (extended near-infrared) obtained upon femtosecond flash photolysis (387 nm) of **PcG3**/SWNT in D_2O with several time delays between 0 and 200 ps at room temperature; see figure legend for details about the time progression. (Bottom) Time-absorption profiles of the femtosecond spectra at 565, 625, 955, 1005, and 1135 nm, monitoring the charge separation and charge recombination.

840 nm resemble the fingerprints of phthalocyanines that are one-electron oxidized by means of electrochemistry and pulse radiolysis.[24] Minima at 630 and 730 nm further accompany these maxima. Important also is the range beyond 1000 nm, where features at 1140, 1270, 1395, and 1530 nm evolve. In the case of 387, 660, and 775 nm excitation the latter are formed at the expense of the decaying SWNT excited state (i.e., 1130, 1170, 1460, and 1535 nm). A global analysis of the 400−1300 nm region resulted in a lifetime of this newly generated state of about 250 ps.

(24) Quintillani, M.; Kahnt, A.; Wölfle, T.; Hieringer, W.; Vázquez, P.; Goerling, A.; Guldi, D. M.; Torres, T. *Chem.—Eur. J.* **2008**, *14*, 3765.

Conclusions

In summary, we have documented through the complementary use of spectroscopy and microscopy mutual interactions between semiconducting SWNT and either a strong electron acceptor, perylenediimide, or a strong electron donor, phthalocyanine. One milestone is the establishment of a versatile methodology to achieve water-soluble SWNT for processing under environmentally friendly conditions. Importantly, the stability of the perylenediimide/SWNT electron donor−acceptor hybrids decreases with increasing dendrimer generation. Two effects are thought be responsible for this trend. With increasing dendrimer generation we enhance(i) the hydrophilicity and (ii) the bulkiness of the resulting perylenediimides. Both effects are synergetic and, in turn, lower the immobilization strength onto SWNT. On the other hand, in phthalocyanine/SWNT electron donor−acceptor hybrids the larger size of the phthalocyanines relative to that of the perylenediimides seem to overcome, in part, the dendron bulkiness. Another milestone is that a wide range of complementary spectroscopies confirmed that distinct ground- and excited-state interactions prevail and that kinetically and spectroscopically well-characterized radical ion pair states are formed. Ground-state interactions are limited to $\pi-\pi$ stacking as evidenced by Raman spectroscopy without giving rise to either p- or n-doping.

Experimental Section

Syntheses. The synthesis of dendritic branches **1**−**2**[19] and free base phthalocyanines **PcG1**−**G3** has been accomplished according to literature procedures.[18] Synthetic details and analytical data of the perylene dendrimers **PerG1**−**G2** under study here are provided in the Supporting Information.

Spectroscopy and Microscopy. Steady-state UV/vis/NIR absorption spectroscopy was performed by a Lambda 19 (Perkin-Elmer) or a Cary 5000 spectrometer (VARIAN). Transient absorption spectroscopy was performed with a Clark MRX fs-Lasersystem CPA 2101 (1 kHz, 150 fs pulse width, 775 nm) and the TAPPS system Helios from Ultrafast systems. Steady-state fluorescence spectra were taken from samples by a FluoroMax3 spectrometer (HORIBA) in the visible detection range and by a FluoroLog3 spectrometer (HORIBA) with a IGA Symphony (512 mm × 1 mm × 1 μm) detector in the NIR detection range. Emission lifetimes were determined via time-correlated single-photon counting (TC-SPC) by a FluoroLog3 spectrometer with a MCP detector (R3809U-58). The Raman spectra were run with a FT-Raman spectrometer RFS100 from Bruker with an excitation wavelength of 1064 nm and a liquid nitrogen-cooled Germanium detector. AFM images were taken by an AFM microscope SolverPro M from NT-MDT.

Acknowledgment. Funding from MEC (CTQ2008-00418/BQU, CONSOLIDER-INGENIO 2010 CDS2007-00010 NANOCIENCIA MOLECULAR, PLE2009-0070), MICINN (FOTOMOL, PSE-120000-2009-008), ESF-MEC (MAT2006-28180-E, SOHYDS), COST Action D35, Comunidad de Madrid MADRISOLAR-2, S2009/PPQ/1533), and Deutsche Forschungsgemeinschaft (SFB 583) is acknowledged. U.H. thanks the MEC (Spain) for a "Ramón y Cajal" research contract.

Supporting Information Available: Syntheses and spectroscopic data of perylene dendrimers **PerG1**−**2** as well as photophysical characterization of **PerG1**−**2**/**PcG1**−**3** without SWNT. This material is available free of charge via the Internet at http://pubs.acs.org.

JA100065H